

Kinetics of electrochemical corrosion of silicon wafers in dilute HF solutions

Valérie Bertagna ^a, Christian Plougonven ^a, François Rouelle ^b, Marius Chemla ^{b,*}

^a Laboratoire d'Analyses IBM, F-91105 Corbeil Essonnes, France

^b Laboratoire d'Electrochimie, Université P. et M. Curie, F-75005 Paris, France

Received 30 May 1996; revised 23 July 1996

Abstract

An extensive experimental study of the factors influencing the electrochemical characteristics of the silicon/DHF junction has been undertaken, and leads to reproducible and reliable values of the electrochemical kinetics of the corrosion reactions. The usual model of electron and hole transfers between a semiconductor and an electrolyte solution should include an additional term due to the generation of h^+ and e^- charges resulting from the dual redox reactions on anodic and cathodic sites. Then, in a narrow range of potential near the corrosion conditions, the classical Butler–Volmer electrochemical equations apply.

The values of open circuit voltage and corrosion current have been obtained using n- and p-type silicon with different doping levels, in contact with deoxygenated or oxygen-saturated DHF solution, in the dark and under illumination. These data were used to characterize the electrochemical reaction kinetics leading to the corrosion rate expressed in atoms per square centimeter per second of different Si substrates. In addition, we derived an estimation of the exchange current density of the hydrogen evolution reaction on the Si surface.

Keywords: Silicon; Electrochemistry; Corrosion; Hydrofluoric acid; Hydrogen

1. Introduction

Wafer processing for ultra-large scale integrated circuit (ULSI) technology must guarantee ultra-clean surfaces. The fabrication steps required for device elaboration must improve for performing successful oxidation or epitaxial growth of silicon in the fabrication of MOS devices. It is very important to produce a clean and chemically stable silicon surface which should be free from impurities and any kind of defect [1]. Surface structures of silicon, including the native oxide or adsorbed elements, are important factors for the quality of the device performance [2]. The wet treatment, RCA cleaning, introduced by Kern and Puotinen [3] in the 1970s, is still used extensively to remove inorganic particles and metallic contamination found on silicon surfaces, and to obtain a stable surface state. Dilute hydrofluoric acid solution (DHF), possibly containing oxidizing additives, is one of the most commonly used cleaning media [4], since it removes the native

oxide layer and results in a stable chemical surface, due to a passivation mechanism. Indeed, chemical reactivity of such a surface is extremely low, as a result of the hydrogen bonding of the surface silicon atoms [5], although these Si–H bonds can be oxidized into Si–OH groups by dissolved oxygen [6].

However, during this treatment some silicon corrosion can occur preferentially at imperfections which act as donors or acceptors. Such effects could result in pitting corrosion which increases the surface roughness, and may then be a source of failure of the final integrated circuits. For example, recent studies demonstrate that roughness is responsible for an increased gate oxide breakdown [7,8]. It is therefore necessary to quantify corrosion processes, and to identify the parameters which govern the corrosion rate, when the silicon sample is simply in contact with the cleaning solution, maintained at its free electrochemical potential.

Several publications deal with the reactivity of silicon wafer surfaces [9–11]. However, most of the authors characterized the formation of surface monohydride silicon groups (Si–H) by infrared techniques [12–15]. In contrast, electrochemical studies often consist of voltammetric mea-

* Corresponding author.

surements, which lie in a wide interval of potential, typically -8 to $+8$ V, although recently Lévy-Clément et al. [10] used a more restricted potential range, i.e. -1 to $+1$ V(SCE). These experimental procedures result in anodic dissolution, within the scale of several tens of milliamps per square centimeter, and then the silicon is seriously etched leading to the formation of porous silicon [16,17]. These structures have been studied for their photoluminescent properties, but they are not consistent with silicon surface smoothness (roughness less than 2 \AA) required in the semiconductor industry.

The corrosion kinetics of silicon wafers in contact with pure DHF solutions can be determined by the mixed potential and the polarization resistance resulting from electrochemical reactions on anodic and cathodic sites; but these processes are very sensitive to so many parameters (structural and impurity defects of the Si surface, dissolved oxygen or metal ions in DHF solutions, organic compound adsorption, etc.) that Föll [18] was led to the conclusion that the zero current potential was ill-defined and not reproducible within a few hundred millivolts.

The goal of the present program is to obtain reproducible and reliable values of the rest potential of n- and p-type silicon samples in contact with DHF. Moreover, the determination of the polarization resistance leads to the knowledge of the corrosion current which can be expressed as the number of dissolved Si atoms per unit of time and surface. The values obtained under various experimental conditions are important parameters for the characterization of both silicon surface state and chemical reactants, involved in industrial applications.

2. Experimental

In a series of preliminary experiments, we used an electrochemical cell as described in a recent publication [19], this cell being of the type usually encountered in electrochemical studies on silicon materials [20,21]. However, the first measurements of open circuit voltage were not reproducible within a few hundred millivolts, as was already pointed out by Föll [18]. It was then necessary to improve this device to have better control of several factors which could be a source of irreproducibility, for example trace amounts of impurities, residual dissolved oxygen, tightness to external light, preliminary chemical treatment of the sample, effect of liquid confinement between the sample and the O-ring seal, etc.

The new electrochemical cell was mainly constituted of a Teflon® vessel, pressed upon the silicon active face between two polyvinyl plates. The whole cell is protected against room light by means of a box made of black polyvinyl polymer. A hole on the cover allows illumination with visible light by means of an optical fiber device, whose intensity was found equal to ca. 1400 lux, as measured with a luxmeter.

The input impedance of the potentiostat being more than $10^{10} \Omega$, the electrical contact on the rear face of the silicon wafer can be obtained simply with a gold foil; the contact resistance of the interface Au|Si was found to be less than 100Ω . However, as our procedure includes voltammetric studies with current density reaching several microamps, the electrical contact was made of a Ga + In alloy layer deposited on the silicon backside, connected to the gold foil. Then the contact resistance was less than 1 to 5Ω depending on the substrate.

The counter electrode was a small platinum plate, the reference being a saturated calomel electrode connected to the electrolyte by means of a bridge made of a Teflon® capillary tube filled with a solution of KCl in agarose gel. Electrochemical parameters were determined with a Tacussel Radiometer Analytical PGS 201T potentiostat. This device was driven by an IBM PC computer using the Voltmaster Software, which includes several electrochemical programs such as chronopotentiometry at constant current, zero current open circuit voltage, polarization resistance, cyclic voltammetry, etc. For each run, numerical data were recorded in memory files in the same computer, and used either for drawing the corresponding graphs, or for a mathematical simulation treatment leading to the validation of an interpretation model.

Silicon wafers, 125 mm diameter and $625 \mu\text{m}$ thick, were purchased from MEMC Electronic Materials. The influence of the doping level could be examined by using two kinds of material for each p-type or n-type silicon:

P1: p-type wafers, boron doped, resistivity 1.85 to $3.6 \Omega \text{ cm}$ ($5 \times 10^{16} \text{ at. cm}^{-3}$);

P2: p-type wafers, boron doped, resistivity 11 to $25 \Omega \text{ cm}$ ($10^{15} \text{ at. cm}^{-3}$);

N1: n-type wafers, phosphorus doped, resistivity 1.8 to $2.6 \Omega \text{ cm}$ ($2 \times 10^{16} \text{ at. cm}^{-3}$);

N2: n-type wafers, phosphorus doped, resistivity 20 to $40 \Omega \text{ cm}$ ($2 \times 10^{14} \text{ at. cm}^{-3}$).

These wafers were CZ (100) oriented, one face was mirror polished for CMOS applications, and the backside was treated mechanically as enhanced gettering to establish an ohmic contact. In our experiments, the silicon samples were cleaned beforehand with a mixture of 60% pure H_2SO_4 , 12% H_2O_2 and 28% H_2O at 80°C for 10 min. In semiconductor industry, this cleaning solution allows organic surface impurities to be oxidized, and a new silicon oxide layer to be grown. The sample is then rinsed thoroughly with deionized water and cleaned with DHF solution, leading to a pure oxide-free silicon hydrophobic surface stabilized by a layer of Si-H bonds.

The DHF solutions, 5% by volume, were obtained after mixing 40% HF SLSI grade (metallic element concentration below 1ppb) with pure deionized water, having a resistivity better than $18 \text{ M}\Omega$, produced in the IBM site facilities. Before each series of experiments, the DHF electrolyte, stored in a reserve tank, was deoxygenated by bubbling pure argon gas, N60 grade, containing less than

0.1 ppm residual oxygen for at least 2 h. On the contrary, in order to examine the influence of dissolved O_2 gas under repeatable conditions, another series of experiments was undertaken using the DHF solution saturated (40 ppm) with pure oxygen gas, N55 grade, at atmospheric pressure. In these conditions, the composition of the electrolyte was perfectly defined.

Nearly all experiments were carried out at 20°C.

3. Results

From the large number, about 200, of experimental sets, we concluded that this electrochemical cell, coupled with the experimental method described above, allows reproducible open circuit potential (E_r) and polarization resistance (R_p) measurements, and also reliable linear voltammetric diagrams.

The open circuit potential E_r is the mixed potential the silicon sample attains spontaneously when it is simply immersed in electrolyte. Indeed, silicon in contact with an electrolyte develops cathodic and anodic sites on its surface, which can react with the electrolyte oxidizing and reducing species. The mixed potential gives information about the relative reactivity of these surface sites, and about their variation induced by modifying doping type or electrolyte composition. Moreover, it is very sensitive to trace amounts of surface defects such as impurity contaminants.

In addition, the voltammetric method, in the narrow range of potentials ∓ 50 mV near E_r , is interesting for polarization resistance (R_p) measurement near the zero current point and consequently for silicon corrosion current determination. In most of these experiments, the observed current values lie in the range 100 to 200 nA. In the method used, the software that controls the experiment limits the current to a maximum value of ∓ 500 nA (∓ 200 nA cm⁻²). One cycle was achieved in 1 min. The advantage of such a method is that the electrical current generally shows a linear relationship versus potential, because of the small overvoltage imposed on the system. Moreover, the sample surface is maintained intact.

When extended to a ∓ 250 mV potential range around the rest potential, voltammetric curves can deliver valuable data about the anodic and cathodic processes on the silicon surface, because they lead to a good estimation of the separate oxidation and reduction components of the overall reaction. The method was particularly useful to determine the influence of the charge carriers, or of the presence of oxidizing species.

The electrochemical curves were recorded on numerical files and the corresponding graphs were printed. The Voltmaster program is able to execute successive sequences. The scheme adopted here for each silicon wafer in DHF deoxygenated or oxygenated was the following.

1. Open circuit potential measurements in the dark, 2 min long.

2. Voltammetric measurements in the dark ($j = f(E)$) for three cycles.

3. Open circuit potential measurements under 1400 lux intensity light.

4. Voltammetric measurements under the same light intensity.

Records of open circuit potential versus time are shown in Fig. 1(a) and Fig. 1(b) to illustrate the stability of the measurements and the effect of photon flux at the silicon|electrolyte interface. In Fig. 1(a), P2-Si type silicon was in contact with deoxygenated 5% DHF, kept in the dark during the first minute of the experiment, then illuminated for a few seconds and then again in the dark, in order to show the reversibility of the effect. Fig. 1(b) shows the behavior of an N2-Si type sample, obtained in an oxygen-saturated 5% DHF solution, with the same experimental procedure. These data reveal that both P- and N-type silicon exhibit immediate photopotential responses, of opposite sign and instantaneously reversible when the light is switched off. Indeed, the open circuit potential of p-Si in contact with thoroughly deoxygenated DHF in the dark was about -620 mV(SCE). In that case, the photopotential upon illumination may reach $\Delta E = +440$ mV, such that the value of illuminated p-Si was nearly -180 mV(SCE) (Fig. 1(a)). In contrast, if the HF solution was saturated with pure O_2 gas, the open circuit potential

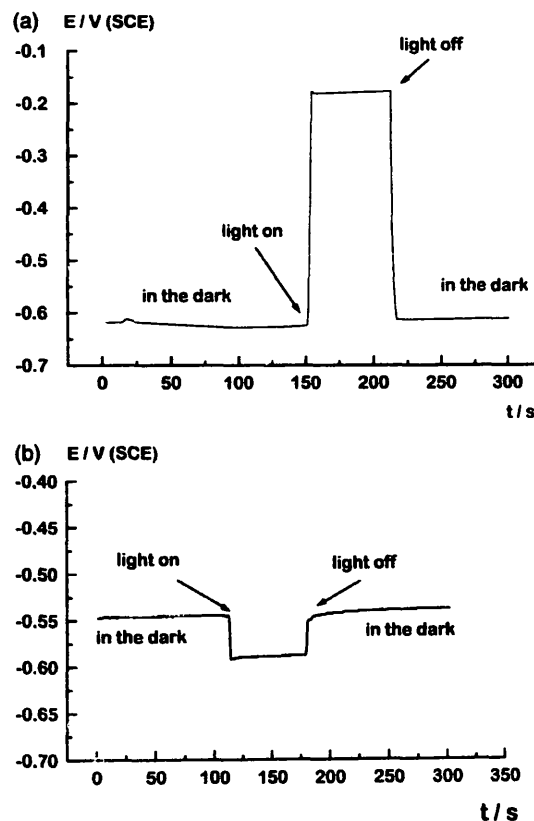


Fig. 1. Potential versus time record in the dark and under light of (a) p-type silicon immersed in 5% deoxygenated DHF and (b) n-type silicon immersed in 5% oxygen-saturated DHF.

Table 1

Electrochemical measurements, open circuit potentials, polarization resistance and dissolved oxygen number when silicon wafers are in contact with deoxygenated 5% DHF

		E_r /mV (SCE)	R_p /k Ω cm ²	j_{corr} /nA cm ⁻²	10^{-11} (dN/dt)/ at. cm ⁻² s ⁻¹
P-Si1	in the dark	-633	2430	5.28	0.33
	with light	-152	101	127	7.93
P-Si2	in the dark	-616	691	20.5	1.28
	with light	-188	131	98	6.12
N-Si2	in the dark	-672	294	43.6	2.72
	with light	-710	52.4	245	15.3
N-Si1	in the dark	-695	118.6	108	6.75
	with light	-695	77	166	13

was only -500 mV, and then the photopotential was $\Delta E = +350$ mV and the open circuit potential under illumination was close to -150 mV(SCE).

In the case of n-type Si, the photopotential ΔE was always negative; however, its value was rather small. We observed that, when n-Si was in contact with deoxygenated DHF, the open circuit potential reached a somewhat more negative value than for p-type. In this case, the photoelectrochemical increment was hardly observed; but, when the rest potential of n-type Si was made more positive by O₂ saturation of the solution, a net photopotential was observed, the value of which was $\Delta E \approx -40$ mV (Fig. 1(b)). This result indicates that surface reactivity of anodic and cathodic sites was immediately modified by photon flux. This effect was reversible.

This photoeffect was recorded on each silicon type, and is given in Tables 1 and 2, where experimental measurements of E_r and R_p with deoxygenated and oxygen-saturated DHF are reported respectively in the dark and under illumination. Fig. 2 represents an example of a voltammogram of P2-Si, in the narrow range of ± 50 mV near E_r in de-aerated DHF in the dark, and shows the linear relationship of j vs. E , leading to a value of $R_p = 690$ k Ω .

Current potential curves give the polarization resistance

Table 2

Electrochemical measurements, open circuit potentials, polarization resistance and dissolved silicon atom number when silicon wafers are in contact with oxygenated 5% DHF

		E_r /mV (SCE)	R_p /k Ω cm ²	j_{corr} /nA cm ⁻²	10^{-11} (dN/dt)/ at. cm ⁻² s ⁻¹
P-Si1	in the dark	-445	538.5	23.8	1.48
	with light	-135	1.66	7730	483
P-Si2	in the dark	-515	625	18.5	1.15
	with light	-158	17	755	47.2
N-Si2	in the dark	-557	91	140	8.75
	with light	-610	10.8	1200	75
N-Si1	in the dark	-568	65	197	12.3
	with light	-603	47	273	17

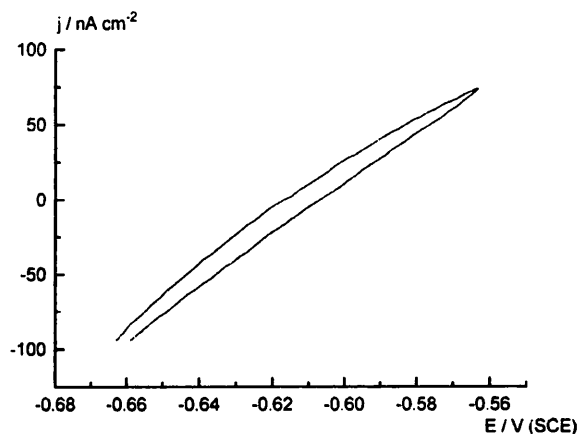


Fig. 2. Voltammogram of p-Si in the narrow range of ± 50 mV near E_r in de-aerated DHF, in the dark.

R_p by measuring the slope $\delta E / \delta j$ near zero current. Indeed, R_p is a function of the corrosion current j_{corr} [22]:

$$R_p \approx RT / (nFj_{\text{corr}}) \quad (1)$$

Formally, n is the number of electrons involved in the transfer, but following Weiss [23] the kinetics of multi-electronic transfers are generally controlled by a 'one-electron-at-a-time' activated step. Owing to the very slow rate of the electron transfer, we have assumed $n = 1$ in the treatment of our data.

The corrosion current leads to a kinetic evaluation of silicon dissolution in DHF, which is equal to the hydrogen evolution reaction. In Tables 1 and 2 are reported experimental measurements of polarization resistance recorded on both p- and n-type silicon, in oxygen-free and oxygen-saturated (40 ppm) DHF solutions, in the dark as well as under illumination. These experimental values show clearly that dissolved oxygen in DHF reduces the polarization resistance. From these observations, we conclude that dissolved oxygen reacts with silicon surface atoms despite the passivation by silicon hydride bonds [38]. In Tables 1 and 2 we have listed corrosion current densities j_{corr} , also expressed as the number of dissolved silicon atoms per unit area and time. Silicon was dissolved in any case, and corrosion current values lie in a range between ten nanoamps and a few microamps. In many publications [24], silicon dissolution is supposed to involve holes (positive charges) which allow covalent silicon bonds to be broken, but our results suggest that N-type silicon is dissolved even in the dark [25].

Under light and with dissolved O₂, the more reactive silicon is P1-type which has the highest p-type doping level. Silicon is then consumed at a rate of 4.8×10^{13} at. cm⁻² s⁻¹, i.e. one silicon monolayer (10^{15} at. cm⁻²) is dissolved each 20 s, assuming that corrosion proceeds uniformly over the surface.

Voltammetric curves in the range of ± 250 mV around the open circuit potential follow a Tafel-like behavior. We present here a few examples of voltammetric curve super-

positions (Figs. 3 and 4) in order to compare the influence of dissolved oxygen or light irradiation respectively. These figures concern N1-type silicon. Fig. 3 shows, for comparison, voltammetric curves obtained with n-type silicon, in the dark, in contact with oxygen-free and oxygen-saturated DHF solutions. In this case, the anodic behavior was almost the same but the cathodic current was amplified by a factor of 10 when DHF contains dissolved oxygen. Fig. 4 shows the behavior of n-Si in contact with oxygen-saturated 5% DHF solution with and without illumination. We can see that the anodic current increased steeply under illumination, as expected from the generation of positive minority carriers. However, we observed that the cathodic branch, corresponding to the reduction of both H^+ ions and O_2 molecules, was also enhanced by the photoelectrochemical process.

These results appear to be proof that dissolved oxygen contributes to the cathodic current as pointed out by Ogawa et al. [6]. These experiments are quite important because, in the semiconductor industry, the content of dissolved oxygen in DHF is not a controlled or well-defined parameter.

One preliminary remark arising from the observed experimental values is that the open circuit potential shifts towards more negative values when the electron carrier density is higher, as indicated by the doping level. This feature was observed with both oxygen-free and oxygen-saturated DHF. This observation was verified many times, since the measurements were well reproducible. Such a result was rather unexpected because n-type semiconductors should exhibit a higher reactivity for electron transfer reactions. In the present experiments, only the reduction of protons or oxygen molecules could be involved, and would then lead to a shift of the mixed potential towards more positive values. The observed results suggest that the states responsible for the exchange current should include not only electronic states but also chemical bonding of surface silicon atoms. This interpretation is supported by the fact that the results of polarization resistance for n-Si are less than those for p-Si. On the contrary, the positive shift of

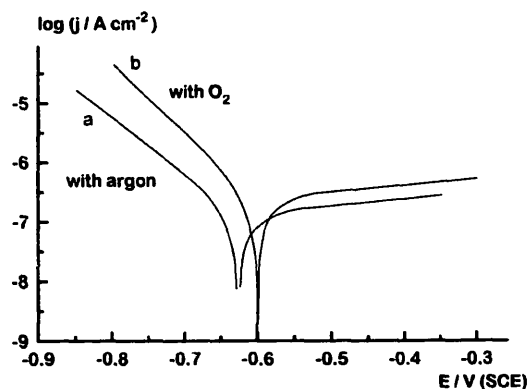


Fig. 3. Voltammetric curve of n-type silicon, in the dark, in contact with deoxygenated and oxygen-saturated DHF respectively for comparison.

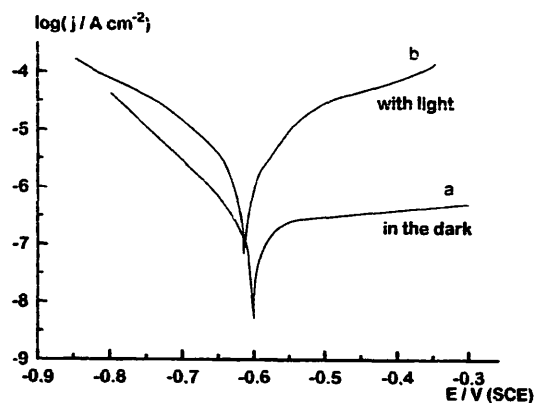


Fig. 4. Voltammetric curve of n-type silicon in contact with oxygen-saturated DHF, in the dark and under light respectively.

potential induced by dissolved oxygen is in good agreement with an electrochemical model, since the cathodic current is increased by the reduction of O_2 molecules [26]. This interpretation will be discussed later.

4. Discussion

The interpretation of our experimental results starts from the general electronic properties of semiconductors as described by Gerischer [26,27], Morrison [28] and Pleskov and Gurevich [29]. An intrinsic semiconductor is not a good conductor. However, when it is p-type or n-type doped, it becomes a conductor with holes (h^+) or electrons (e^-). Immersed in an electrolyte containing redox species, the semiconductor exchanges electrical charges (h^+ and e^-) with ionic species, to achieve the thermodynamic equilibrium.

For a single redox couple in the classical model, the rate of electron transfer is considered to be proportional to the density of carriers in the solid. The basic equations for charge transfer include the density of states both in the semiconductor and in the solution; the rate of the reaction equals the probability of exchange between states at the same level. The formal equation can be presented as a simplified formula as follows. For example, the cathodic current density at a p-type semiconductor is

$$j_c = -ze k_c n_s c_{ox} \exp(-U_c/kT) \quad (2)$$

where k_c is a rate constant, n_s the electron density at the surface, and U_c the activation energy for the cathodic reaction. In semiconductors, the important effect of a voltage change is to influence the density of charge carriers h^+ or e^- at the surface of the electrode; the potential drop through the Helmholtz layer should be negligible. The band edges do not move relative to the energy levels in solution. In these conditions, the apparent transfer coefficient: β_c should be equal to 1 for the direct reaction and 0 for the reverse transfer.

Following Brattain and Garrett [30] and Dewald [31], the charge carrier concentration at the surface of a p-type

semiconductor is controlled by the total consumption j_n of electrons, which is equal to the flow j_i of electrons from the interior plus the contribution j_s of surface generation:

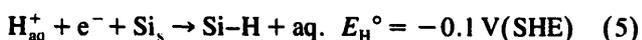
$$j_n = j_i + j_s \quad (3)$$

In Gerischer's treatment of the steady state of the potential distribution $\varphi(x)$ within the space charge region, the Poisson equation should be written

$$j_n = D_n [dn/dx - 1/\Phi d\varphi/dx] - g_s \quad (4)$$

where g_s is the generation rate of electrons at the surface, and $\Phi = kT/e$ is called the thermal volt equivalent.

The term g_s plays an important role in the case of Si in contact with DHF solution, because the electrochemical system corresponds to a mixed potential resulting from the corrosion of the material following two distinct heterogeneous reactions. When DHF is deoxygenated:



the above reaction (6) being followed by successive electrochemical and chemical steps leading to $[\text{SiF}_6]^-$ ion in solution, following the mechanism proposed by Rieger and Kohl [32]. The value $E_{\text{Si}}^\circ = -1.2 \text{ V(SHE)}$ was derived by Sillen [33] from the standard potential of formation of SiO_2 plus the term coming from $[\text{SiF}_6]^-$ complex formation; this result has recently been confirmed [34]. Reactions (5) and (6) are written only as an indication of the current exchange process, but have no meaning with respect to the real mechanism of the transformation. In fact, it is well known that the Si surface is passivated by a quite continuous sheet of Si-H termination bonds, which induce a strong hindrance for the charge transfer. But the electrochemical transfer corresponding to reactions (5) and (6) still exists with a low value of the current density, less than

$1 \mu\text{A cm}^{-2}$. The residual reactivity of the Si substrate is connected with the hole generation g_s at the surface. Recalling that a hole is a missing valence electron, the presence of a hole at the surface means that one of the valence bonds between the surface atom and the rest of the crystal is broken [28]. Capture of holes by surface atoms can lead to soluble species because the gain in solvation energy is greater than the loss in bonding energy.

In a corrosion process, the mixed potential derives from two different reactions with a potential interval of $E_{\text{H}}^\circ - E_{\text{Si}}^\circ \approx 1 \text{ V}$. It is likely that the protons in solution can exchange electrons with the conduction band of the semiconductor, while Si atoms can capture holes from the valence band. We must point out that this dual redox system acts as a source g_s of surface carriers on the semiconductor. For example, electrochemical reaction (5) consumes electrons (or generates holes), while reaction (6) consumes holes only at the surface of the silicon electrode (Fig. 5). If the equilibrium concentration of both carriers is disturbed, then new carriers are generated by thermal fluctuations.

In the vicinity of zero current potential, the capture of electrons by a proton discharge reaction may generate enough surface holes for the potential drop in the space charge region to be rather small, and Eq. (2) to approach a Butler–Volmer relationship:

$$j_+ = j_+^0 \exp(\beta_2 \eta_{\text{h}}/\Phi) = j_+^0 \exp[\beta_2(E - E_{\text{Si}})/\Phi] \quad (7)$$

A symmetrical argument could lead to the voltage dependence of proton reduction reaction

$$\begin{aligned} j_- &= -j_-^0 \exp[-(1 - \beta_1) \eta_{\text{h}}/\Phi] \\ &= j_-^0 \exp[-(1 - \beta_1)(E - E_{\text{H}})/\Phi] \end{aligned} \quad (8)$$

where β_1 and β_2 are the transfer coefficients of the H and Si electrochemical reactions respectively.

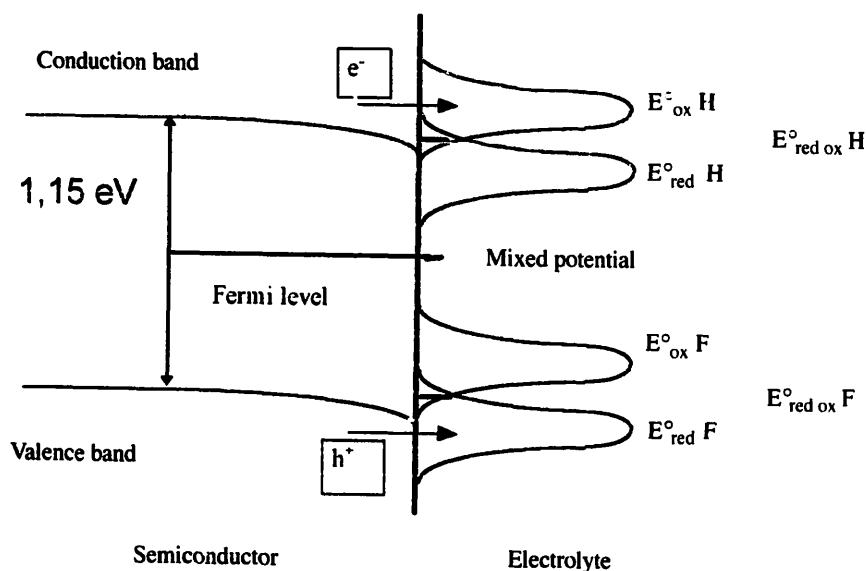


Fig. 5. Energy band diagram of the semiconductor|electrolyte junction when the electrolyte contains two redox couples.

When current flow increases, the contribution of minority carrier transport overvoltage becomes more important, and the current voltage relationship approaches Eq. (4). The current from the interior to the space charge layer is approximately

$$-j_i = eD_n(n_o - n_i)/L \quad (9)$$

where D_n is the diffusion coefficient of electrons in silicon, and L the free diffusion length of the electron. The current then reaches a saturation value

$$-j_{\text{sat}} = D_n n_o / L \quad (10)$$

For a p-type semiconductor, the expression of j_- should be modified to [26]

$$j_- = j_-^\circ (1 - j/j_{\text{sat}}) \exp[-(1 - \beta_1)(E - E_H)/\Phi] \quad (11)$$

Now, provided the scanned potential range remains between E_H and E_{Si} , the generation of electrons and holes by both redox reactions continues to contribute to decrease the potential drop within the space charge region, whose influence should result simply in a change of the apparent transfer coefficients β_1 and β_2 .

On a fundamental basis, these arguments support the use of a Butler–Volmer current–potential relationship [35], as was also indicated by Pleskov.

From the above equation, the partial current, under open circuit conditions, gives a value which can be identified as the corrosion current:

$$\begin{aligned} j_{\text{corr}} &= j_+^\circ \exp[\beta_2(E_r - E_{\text{Si}})/\Phi] \\ &= j_-^\circ \exp[-(1 - \beta_1)(E_r - E_H)/\Phi] \end{aligned} \quad (12)$$

Then

$$E_r = \Phi \ln(j_-^\circ / j_+^\circ) + 0.5(E_{\text{Si}} + E_H) \quad (13)$$

In contrast, the slope $\delta j / \delta E$ close to the open circuit voltage is

$$(\delta j / \delta E)_{j=0} = 1/R_p \approx \sqrt{(j_+^\circ j_-^\circ)} \exp[(E_H - E_{\text{Si}})/4\Phi] \quad (14)$$

assuming β_1 and β_2 are approximately equal to 0.5.

Our experimental data lead to the determination of the corrosion current, which can be expressed in microamps per square centimeter as well as in number of dissolved atoms per square centimeter per second. Secondly, we can also determine the two unknown parameters j_+° and j_-° which characterize the two redox reaction kinetics.

In our study, we have obtained many experimental results using N_1 , N_2 , P_1 , P_7 silicon samples, in contact with deoxygenated and oxygen-saturated DHF solutions, in the dark and under illumination. The reproducibility of results was also examined. Results reported in Fig. 1(a), Fig. 1(b), Fig. 3, and Fig. 4 are cited as examples, and show that the above electrochemical interpretation applies to all these experimental results which, in turn, sustain the electrochemical model.

Under all experimental conditions, only one reaction can occur on anodic sites. It corresponds to Si element dissolution following reaction (6), although the real detailed mechanism cannot be derived from our measurements. It can be suggested that the Si–H passivating layer is not perfect and, following the results of Takahagi and coworkers obtained by XPS [36,37], a small fraction of the surface sites is terminated by fluorine or hydroxyl groups. Then



According to commonly accepted mechanisms [24], the first step of Si anodic dissolution is the formation of Si^{II} , which is subsequently converted into Si^{IV} by a dismutation chemical reaction.

In deoxygenated DHF, only one transfer reaction involving protons can occur on cathodic sites. The first step is the formation of Si–H bonds, but the kinetics of corrosion, as confirmed by AFM observations, must include hydrogen evolution:

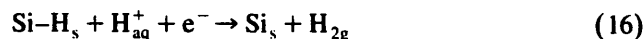


Fig. 3(a) shows the Tafel diagram corresponding to n-Si in de-aerated DHF, in the dark. The cathodic branch is linear with a slope corresponding approximately to $\beta_c n \approx 0.5$. The anodic branch has an apparent $\beta_a n$ near 0.2, but the current tends to limit at j_{sat} because of the small concentration of holes in n-type crystals.

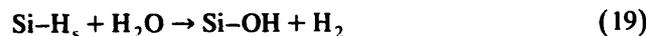
When DHF is oxygenated, a second reaction on cathodic sites is involved:



Alternatively



Again reactions (17) and (18) cannot be considered as describing a real mechanism. It is likely that the reaction proceeds through the intermediate formation of Si–OH terminal bonds. Silicon is known to be oxidized in ambient air containing O_2 molecules [38] or in water [39]. Water molecules are supposed to break silicon covalent bonds to form hydroxyl groups on the silicon surface. This reaction can proceed on Si–H or Si–F sites.



or



Fig. 3(b) represents the Tafel diagram of n-Si, in the dark, in oxygenated DHF. The curve shape is similar to that in Fig. 4(a). It is interesting to note that the saturation current on the anodic branch attains approximately the same value as for deoxygenated solution, thus supporting the statement of a limitation by hole concentration. But the rest potential is shifted to more positive potentials as a result of a steep increase of the reduction current on the

cathodic branch. For each value of the potential the current density is almost ten times higher for O_2 than for proton electrochemical reduction.

The effect of light illumination was shown by our experimental data (Fig. 4). As expected, the transfer reaction of minority carriers was found to be amplified. This phenomenon was already known [40], and is a characteristic of semiconductor electronic properties. However, in our experimental results we also observed that both anodic and cathodic currents were increased. Naturally, as a consequence of electroneutrality, light generates electron–hole pairs. Although essentially the density of minority carriers is strongly affected, we can think that, depending upon light intensity [40], majority carriers are also created at a non-negligible level.

As indicated by Eq. (13), the open circuit potential is strongly dependent on the relative intensity of anodic and cathodic currents. The effect appears very clearly upon illumination of p-type silicon in contact with DHF solutions, as the reduction current is highly amplified by the photogenerated e^- minority carriers. The effect is so large that the potential under light is around -150 to -180 mV(SCE), compared with the value of -620 to -640 mV in the dark.

Illumination of n-type silicon results in the amplification of both anodic and cathodic branches. Moreover, the relative amplification of anodic current by light is much less, by a factor of 100, than the amplification of cathodic current on p-Si. This feature explains why the negative potential increment observed with n-Si is so small. It could be interpreted by the assumption that the passivating layer of Si–H terminal bonds should be more effective against the silicon dissolution than against the hydrogen evolution reaction.

Another consequence of the generation of minority carriers is illustrated in Fig. 4, which shows that not only is the anodic current density amplified, but moreover the apparent transfer coefficient β_a is modified to attain a 'normal' value of about 0.5. This is another argument for assigning the slope of the anodic branch to the influence of j_{sat} in the case of n-Si in the dark.

Finally, from the computation of experimental results, mainly the open circuit potential, transfer resistance and voltammetric data, using Eqs. (12) and (13), it was possible to derive an estimate of the exchange current for proton reduction at the equilibrium potential in the DHF solution. Naturally, these quantitative results can only be approximate because of the long-range extrapolation procedure. The following values were obtained from our computations for the different Si samples, in the dark and under illumination:

1. In the dark.

- P-Si1 $j_H^0 = 2.8 \times 10^{-11} \text{ A cm}^{-2}$
- P-Si2 $j_H^0 = 1.4 \times 10^{-10} \text{ A cm}^{-2}$
- N-Si1 $j_H^0 = 1.1 \times 10^{-10} \text{ A cm}^{-2}$
- N-Si2 $j_H^0 = 1.8 \times 10^{-10} \text{ A cm}^{-2}$

2. Under illumination.

- P-Si1 $j_H^0 = 8.0 \times 10^{-6} \text{ A cm}^{-2}$
- P-Si2 $j_H^0 = 3.0 \times 10^{-6} \text{ A cm}^{-2}$
- N-Si2 $j_H^0 = 2.7 \times 10^{-10} \text{ A cm}^{-2}$
- N-Si1 $j_H^0 = 3.0 \times 10^{-10} \text{ A cm}^{-2}$

These data can be considered as in agreement with earlier published values [41], and are useful to complement the values of the proton exchange current on an Si single crystal as given by Appleby et al. [42]. Finally, these last results can contribute to our knowledge of the hydrogen evolution reaction.

5. Conclusions

The experimental procedure we have developed to study the silicon|electrolyte interface allows electrochemical parameters to be measured in a precise, reproducible and reliable way. In turn, the experimental results and their interpretation support the applicability of an electrochemical model for the silicon|DHF interface as a consequence of the dual redox potential arising from the corrosion reaction.

One of our results is that silicon corrosion is oxygen dependent. We can simply propose that O_2 molecules can break Si–H bonds to oxidize surface silicon atoms. For a rigorous experimental procedure, we used DHF saturated with pure oxygen gas. These experiments are quite interesting because dissolved oxygen in DHF is not a controlled or well-defined parameter in semiconductor industry.

Also, as a result of the reproducibility of our measurements, we could demonstrate that silicon electrochemical properties, measured in 5% DHF, were very sensitive to the presence of dissolved oxygen, light irradiation and, more generally, to the presence of any impurity in the electrolyte or any defect on the substrate surface. We can add that such an electrochemical study should be of great interest for the characterization of the electrode surface state.

Acknowledgements

The authors express their thanks to MEMC Company for providing n- and p-doped silicon wafers.

References

- [1] T. Ohmi, Breakthrough for Scientific Semiconductor Manufacturing in 2001, Realize Inc., Tokyo, 1992, p. 36.
- [2] A.C. Diebold and B. Doris, Surf. Interface Anal., 20 (1993) 127.
- [3] W. Kern and D.A. Puotinen, RCA Rev., 31 (1970) 187.
- [4] J.N. Chazalviel, J. Phys. IV, 4 (1994) C117.
- [5] Y.J. Chabal, G.S. Higashi, K. Raghavachari and V.A. Burrows, J. Vac. Sci. Technol., A7 (1989) 2104.

- [6] H. Ogawa, K. Ishikawa, M. Suzuki, Y. Hayami and S. Fujimura, *Jpn. J. Appl. Phys.*, 34 (1995) 732.
- [7] M.C. Lopes, S.G. dos Santos, C.M. Hasenack and V. Baranauskas, *J. Electrochem. Soc.*, 143 (1996) 1021.
- [8] H. Akiya and M. Itsumi, *J. Electrochem. Soc.*, 143 (1996) 973.
- [9] D.R. Turner, *J. Electrochem. Soc.*, 105 (1958) 402.
- [10] C. Lévy-Clément, A. Lagoubi, R. Tenne and M. Neumann-Spallart, *Electrochim. Acta*, 37(5) (1992) 877.
- [11] P.C. Searson and X.G. Zhang, *Electrochim. Acta*, 36 (1991) 499.
- [12] V.A. Burrows, Y.J. Chabal, G.S. Higashi, K. Raghavachari and S.B. Christman, *Appl. Phys. Lett.*, 53 (1988) 998.
- [13] K. Sawara, T. Yasaka, S. Miyazaki and M. Hirose, *Jpn. J. Appl. Phys.*, 31 (1992) L931.
- [14] J.N. Chazalviel, *J. Electrochem. Soc.*, 138 (1991) 153.
- [15] H. Bender, S. Verhaverbeke and M. Heyns, *J. Electrochem. Soc.*, 141 (1994) 3128.
- [16] P.C. Searson and X.G. Zhang, *J. Electrochem. Soc.*, 137 (1990) 2539.
- [17] I. Ronga, A. Bsiesy, F. Gaspard, R. Herino, M. Ligeon and F. Muller, *J. Electrochem. Soc.*, 138 (1991) 1403.
- [18] H. Föll, *Appl. Phys. A: Solid. Surf.*, 53 (1991) 8.
- [19] L. Torcheux, A. Mayeux and M. Chemla, *J. Electrochem. Soc.*, 142 (1995) 2037.
- [20] S.A. Hendricks, Y.-T. Kim and A.J. Bard, *J. Electrochem. Soc.*, 139 (1992) 2818.
- [21] E. Peiner and A. Schlachetzki, *J. Electrochem. Soc.*, 139 (1992) 552.
- [22] A.J. Bard and L.R. Faulkner, *Electrochimie, Principes Méthodes et Applications*, Masson, Paris, 1983.
- [23] J. Weiss, *Nature*, 137 (1934) 648.
- [24] R. Memming and G. Schwandt, *Surf. Sci.*, 4 (1966) 109.
- [25] F. Gaspard, A. Bsiesy, M. Ligeon, F. Muller and R. Herino, *J. Electrochem. Soc.*, 136 (1989) 3043.
- [26] H. Gerischer, in P. Delahay and C.W. Tobias (Eds.), *Advances in Electrochemistry and Electrochemical Engineering*, Vol. 1, Interscience, New York, 1961.
- [27] H. Gerischer, *Electrochim. Acta*, 35 (1990) 1677.
- [28] S.R. Morrison, *Electrochemistry of Semiconductor and Oxidized Metal Electrodes*, Plenum Press, New York, 1980.
- [29] Yu.V. Pleskov and Yu.Ya. Gurevich, *Semiconductor Photoelectrochemistry*, Consultants Bureau, New York and London, 1986.
- [30] W.H. Brattain and C.G.B. Garrett, *Bell System Tech. J.*, 34 (1955) 129.
- [31] J.F. Dewald, *J. Electrochem. Soc.*, 104 (1957) 244.
- [32] M.M. Rieger and P.A. Kohl, *J. Electrochem. Soc.*, 142 (1995) 1490.
- [33] L.G. Sillen, *Stability Constants of Metal-ion Complexes*, The Chemical Society, London, 1964.
- [34] K. Osseo-Asare, D. Wei and K.K. Mishra, *J. Electrochem. Soc.*, 143 (1996) 749.
- [35] D. Landolt, *Traité des Matériaux. Corrosion et chimie des surfaces de métaux*, Presses Polytechniques et Universitaires Romandes, Lausanne, 1993.
- [36] T. Takahagi, I. Nagai, A. Ishitani and Y. Nagasawa, *J. Appl. Phys.*, 64 (1988) 3516.
- [37] S.R. Kasi, M. Liehr and S. Cohen, *Appl. Phys. Lett.*, 58 (1991) 2975.
- [38] M. Niwano, J. Kageyama, K. Kurita, K. Kinashi, I. Takahashi and N. Miyamoto, *J. Appl. Phys.*, 76 (1994) 2157.
- [39] D. Gräf, M. Grundner and R. Schulz, *J. Vac. Sci. Technol.*, A7 (1989) 808.
- [40] H. Gerischer, M. Lübke and B. Bressel, *J. Electrochem. Soc.*, 130 (1983) 2112.
- [41] E.A. Efimov, I.G. Erusalimchik and G.P. Sokolova, *Zh. Fiz. Khim.*, 36 (1962) 1005.
- [42] A.J. Appleby, M. Chemla, H. Kita and G. Bronoel, in A.J. Bard (Ed.), *Encyclopedia of Electrochemistry of the Elements*, Vol. IX, Marcel Dekker, New York, 1982.